

**EM 388F – Fracture Mechanics**

**The Energy Release Rate and the Effect of  
Free Surface on Stress Intensity Factor in 3D problem**

**Term Paper**

**Spring, 2008**

**Dept. of Aerospace Engineering &  
Engineering Mechanics  
The University of Texas at Austin**

**Suk-Kyu Ryu**

## Abstract

In general fracture theory, stress intensity factor or energy release rate have been obtained through the assumption of 2D problem. In other words, the energy release rate is constant along the crack line(front) in the z direction. However, when we consider a 3D crack problem, the energy release rates value shows a significant drop close to the free surface when compared to the 2D solution. This is considered due to the “free surface effect” when a crack meets a free surface. Precisely, stress intensity factor is zero on free surface and the singularity does not have the classical square-root any more. In this term project, I will show the tendency of energy release rates along the crack front by dint of this free surface effect. So the distribution of energy release rate,  $G$  across the specimen width will be evaluated numerically by ABAQUS/standard and then, the results will be compared to the 2D solution. A double cantilever beam(DCB) specimen is introduced for a numerical solution. The specimen is idealized 3D structure with isotropic material. Finally, I will also explain the process of obtaining the semi-analytic solution for stress intensity factor of the free surface in a half space by introducing the Boussinesq-Papkovich-Neuber functions. This semi-analytic solution shows that at the half-space surface the stress-intensity factor is zero, and stresses are related with poisson's ratio.

*Keywords:* Energy release rate, DCB, Stress intensity factor, Quarter-infinite crack in a half-Space, Boussinesq-Papkovich-Neuber functions

## **I. Introduction**

Fracture analysis and prevention are important functions to all of the engineering fields. So many engineers often play a lead role in the analysis of failures, whether a component or product fails in service or if failure occurs in manufacturing or during production processing. During the past 40 years, linear elastic fracture mechanics (LEFM) has been used for predicting the fracture behavior. However, most analytic or numerical investigators focused on the 2D or axi-symmetric problem. As you can see, the real structure has mostly 3D dimension such that the state of deformation near the crack tip is always three-dimensional. Thus, if we apply 2D linear elastic fracture mechanics, sometimes we can't fully understand the occurrence. To overcome the limit of 2D, some researcher tried to find out the solution for a structure with 3D crack. For a flat plate of finite thickness with a through-the-thickness crack, attempts were made by Hartranft and Sih (1969) to obtain stress distribution close to the crack front, but the closed form solutions were intractable. The profile of stress intensity in the thickness direction was not determined, but the functional form of the stresses was obtained. The functional form showed that stress singularity is the inverse square root type at the crack front. A year later, Hartranft and Sih (1970) proposed an approximate three-dimensional plate theory that approximately satisfies the stress-displacement relations. Later, Benthem showed that at the intersection of the crack front and a free surface, the singularity does not have the classical square-root power but is a function of the material poisson's ratio. Additionally, this results explained why stress intensity factor drop dramatically at the free surface. In this term paper, I showed briefly the process of obtaining his solution.

In recent years, the development of computers can provide better accuracy of solutions in three-dimensional problems involving singularities. In this paper, I also evaluated the energy release rate for 3D crack problem by using ABAQUS[v6.1] and observe the varying trend according to some different factors.

## II. Double Cantilever Beam Specimen

### Analytic Solution

In fracture mechanics, the simplest model, double-cantilever beam (DCB) (Fig 1) for determining the strain energy release rate is used theoretically (Oh et al., 1987; Kook and Dauskardt, 2002). The equation of energy release rate per unit length for homogeneous DCB specimen is given by [1]

$$G_T = \frac{12(Pa)^2}{\bar{E}B^2H^3} \left(1 + 0.677 \frac{H}{a}\right)^2$$

where P means loading forces at the tip of double cantilever, a is delamination length, B is the width of double cantilever, H is the substrate half-thickness and  $\bar{E}$  is elastic modulus. This analytic solution shows that the energy release rate for plane stress is higher than for plane strain since modulus for plane stress is smaller.

### Numerical Solution

In this paper, a double cantilever beam (Fig 1) made of silicon material with distributing load is implemented as a FEA model for a numerical solution. ABAQUS(v6.6-1), one of famous general purpose FEA programs is used to analyze FEA model. Young's modulus for silicon is 130.2 Gpa and poisson's ratio is 0.28

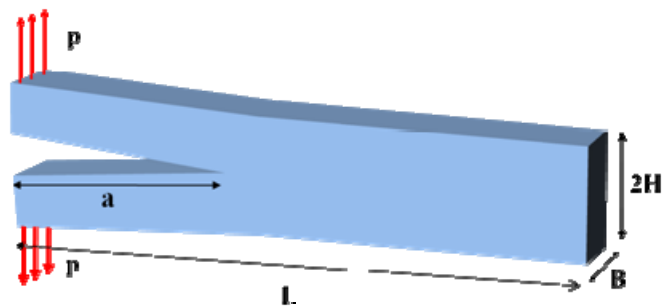


Fig 1. Double Cantilever Beam Specimen

First, different depths( $B$ ) are introduced to investigate the 3D effect along the crack line. It can be expected for the depth expansion to give an effect on the ERRs along the crack line since the variation of boundary condition corresponding to position along the depth would affect the effective modulus and stress. For this numerical model, the length( $L$ ) is fixed as 200mm. Fig 2 indicates that the strain energy release rate for relatively small width shows locally highest pitch value in the middle part of the specimen progressively decreasing towards the edges. However, as the depth is increased, the energy release rates are getting lower near the center of DCB. Usually, the plane stress condition is applied for a thin elastic problem and the plane strain condition is for an infinite case. As mentioned before, the ERR for plane stress is larger than plane strain. Through the Fig 2, we can observe the transition of boundary condition. For a relatively narrow width, the energy release rate shows higher value. Then, as the width is increased, the energy release rate is getting lower. However, when considering the averaged ERRs along the crack line, the mean ERRs pretty accord with one of plane stress/strain (Fig 3). For a relatively thin width, the averaged ERR corresponds to the plane stress and as the width approaches to the infinite, the mean value also translates into ERR for plane strain. Furthermore, the relative effect of delamination length on the width is investigated. For the fixed width(200 mm), normalized ERRs with respect to one of plane stress show clearly the effect of these parameters (Fig 4). The tendency appears similar with the first study for the width effect. From the numerical solution, the relationship between width and delamination length can be explained. If width is much smaller than crack length, the constraint effect of plane strain is activated. Reversely, when width is larger or similar with delamination length, the constraint effect corresponds to the state of plane stress.

Finally, we can observe the energy release rate drops dramatically at the free surface even though some factors are changed. In many numerical solutions for energy release rate, this similar trend can be seen [2]. From next section, I will explain why this happens through the Benthem's semi-analytic solution [3].

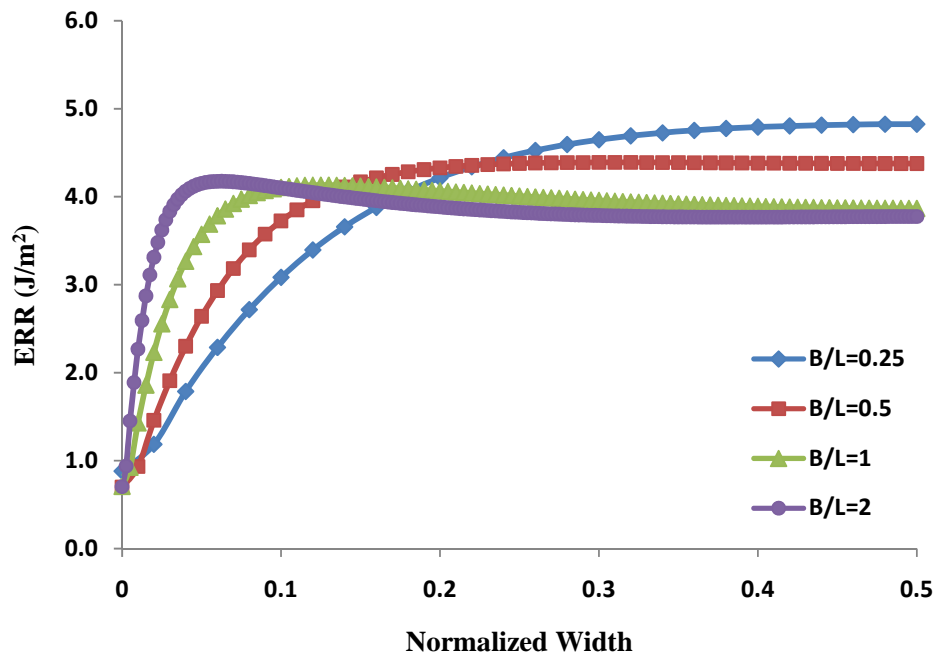


Fig 2. The energy release rate according to different width

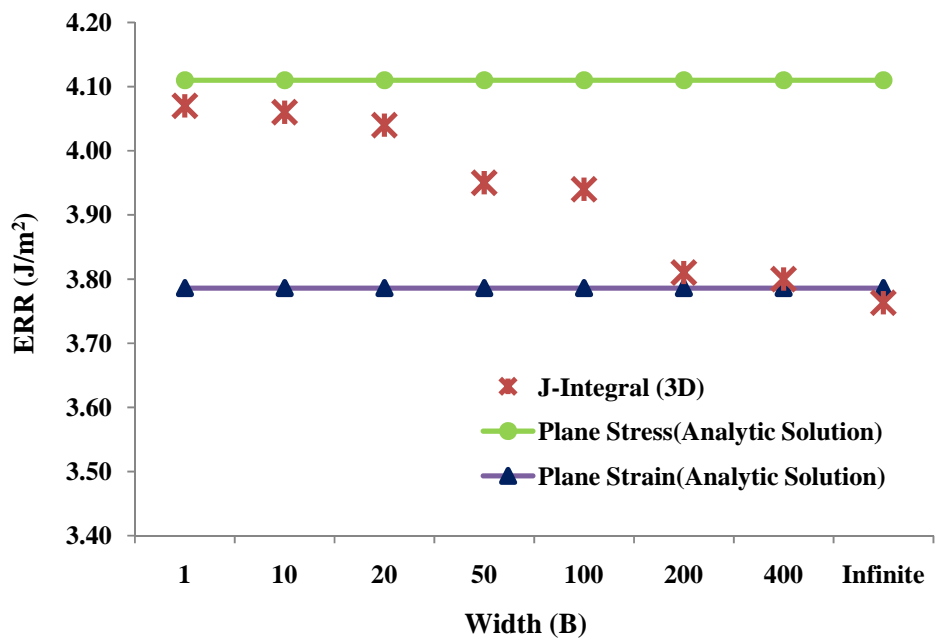


Fig 3. The averaged energy release rate

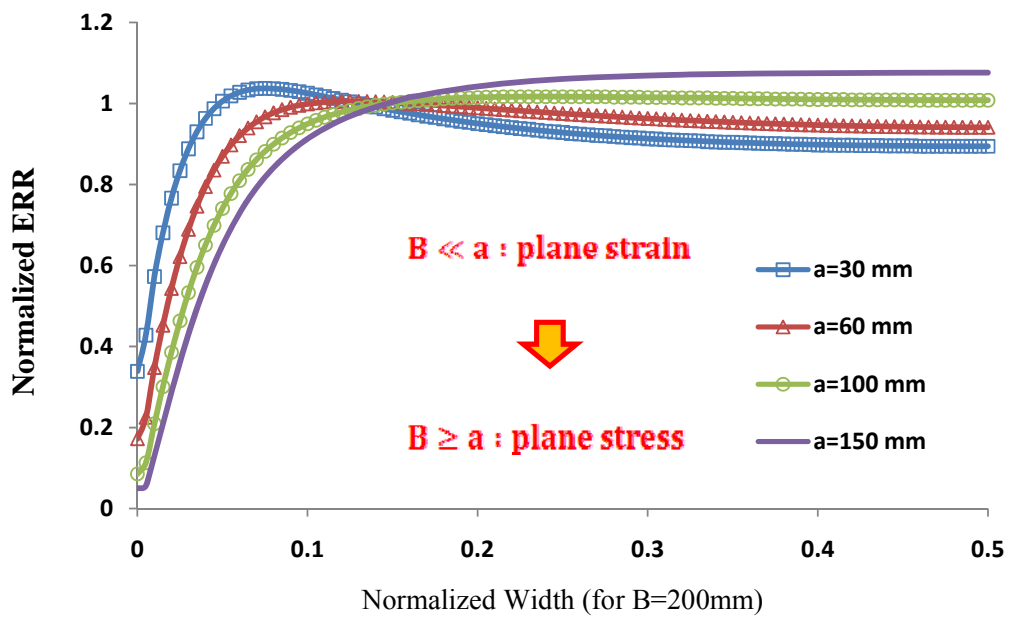
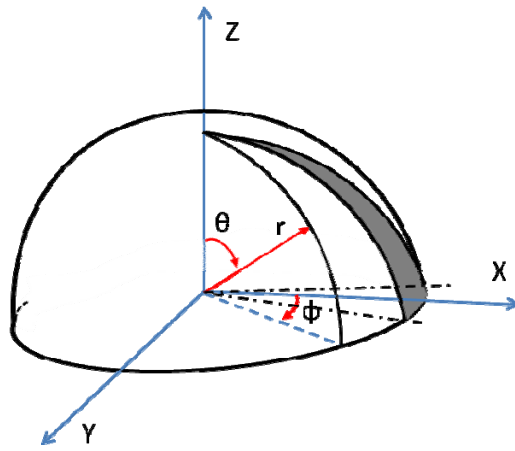


Fig 4. The energy release rate according to different delamination length

### III. State of Stress at the vertex of Quarter-Infinite Crack in a Half-Space

#### Boussinesq-Papkovich-Neuber Stress Functions

The quarter-infinite crack in a half-space is shown in Fig 5. Cartesian coordinates are  $x, y, z$  spherical coordinates are  $r, \theta, \phi$



$$x = r \sin \theta \cos \phi$$

$$y = r \sin \theta \sin \phi$$

$$z = r \cos \theta$$

Fig 5. Quarter-infinite crack in a half-space

The crack occurs in the quarter-plane  $y=0, x>0, z>0$ . The state of stress in the half-space around the crack is

$$\sigma_{xx} = r^\lambda f_{xx}(\lambda, \theta, \phi), \quad \sigma_{xy} = r^\lambda f_{xy}(\lambda, \theta, \phi), \quad \text{etc ...}$$

To find solutions, Boussinesq-Papkovich-Neuber Stress Functions are introduced. Boussinesq created 7 basic solutions of the Navier equations with the aid of harmonic functions [4].

$$\text{(sol. 1)} \quad u = 0, v = \frac{\partial \psi_1}{\partial z}, w = -\frac{\partial \psi_1}{\partial y},$$

$$\text{(sol. 2)} \quad u = \frac{\partial \psi_2}{\partial z}, v = 0, w = \frac{\partial \psi_2}{\partial x}$$

$$\text{(sol. 3)} \quad u = \frac{\partial \psi_3}{\partial y}, v = -\frac{\partial \psi_3}{\partial x}, w = 0$$

$$\text{(sol. 4)} \quad u = \frac{\partial \psi_4}{\partial x}, v = \frac{\partial \psi_4}{\partial y}, w = \frac{\partial \psi_4}{\partial z}$$

$$(sol. 5) \quad u = (-3 + 4\nu)\psi_5 + x \frac{\partial \psi_5}{\partial x}, \quad v = x \frac{\partial \psi_5}{\partial y}, \quad w = x \frac{\partial \psi_5}{\partial z}$$

$$(sol. 6) \quad u = y \frac{\partial \psi_6}{\partial x}, \quad v = (-3 + 4\nu)\psi_6 + y \frac{\partial \psi_6}{\partial y}, \quad w = y \frac{\partial \psi_6}{\partial z}$$

$$(sol. 7) \quad u = z \frac{\partial \psi_7}{\partial x}, \quad v = z \frac{\partial \psi_7}{\partial y}, \quad w = (-3 + 4\nu)\psi_7 + z \frac{\partial \psi_7}{\partial z}$$

## Separation of variables technique

Benthem used the method of separation of variables. He attempted to determine the singular stress distribution in the neighborhood of the vertex of a quarter plane crack using a semi-analytical approach. So seven functions separated into the variables of the spherical coordinate are considered [5].

$$\psi = r^{\lambda+2} \exp(i\mu\varphi) P_{\lambda+2}^{\mu}(\cos \theta)$$

where  $P_{\lambda+2}^{\mu}(\cos \theta)$  is an associated Legendre function of the first kind and  $\mu, \lambda$  may have any complex value.

Starting from the seven basic solutions, the differentiation formulas allow to compute their displacement, strain and stress. However, in this investigation, we limit problem to stress system which are symmetrical with respect to the plane  $\varphi = \pi$ . Thus, these solutions[6] are

$$\text{Sol. A} = \text{sol. 2} \{ \psi_2 = \psi_A \}$$

$$\psi_A = r^{\lambda+2} \exp(i\mu\varphi) P_{\lambda+2}^{\mu}(\cos \theta)/G \quad (\mu = 0, -1, -2, \dots)$$

$$\text{Sol. B} = \text{sol. 1} \{ \psi_1 = (1 - \nu)\psi_A \} + \text{sol. 6} (\psi_6 = \frac{1}{2} \frac{\partial \psi_B}{\partial z})$$

$$\psi_B = r^{\lambda+2} \exp(i\mu\varphi) P_{\lambda+2}^{\mu}(\cos \theta)/G \quad (\mu = -1, -2, -3, \dots)$$

$$\text{Sol. C} = \text{sol. 4} \{ \psi_1 = (\frac{1}{2} - \nu)\psi_C \} + \text{sol. 6} (\psi_6 = \frac{1}{2} \frac{\partial \psi_C}{\partial y})$$

$$\psi_C = r^{\lambda+2} \exp(i\mu\varphi) P_{\lambda+2}^{\mu}(\cos \theta)/G \quad (\mu = -\frac{3}{2}, -\frac{5}{2}, -\frac{7}{2}, \dots)$$

The stress fields obtained satisfy the differential equation, but does not satisfy the free surface boundary conditions in the pointwise sense.

### The approximate weighted residual operator

Therefore, he was forced to apply approximate weighted residual type operators to satisfy the boundary condition. This operation leads to a system of algebraic equations of infinite order, which must be truncated to obtain numerical results. Here the approximate weighted residual operators are

$$\text{On } \sigma_{zx}, \int_0^{2\pi} \dots \cos(n-1) \varphi d\varphi = 0$$

$$\text{On } \sigma_{zy}, \int_0^{2\pi} \dots \sin n\varphi d\varphi = 0$$

$$\text{On } \sigma_{zz}, \int_0^{2\pi} \dots \cos(n-1) \varphi d\varphi = 0 \quad (n = 1, 2, 3 \dots)$$

### Assumption

However, unfortunately this operator also did not succeed in achieving convergence. Therefore, he assumed that the half-space surface ( $z=0$ ) is “struck” by an arbitrary load.

$$\sigma_{zx} = 0, \quad \sigma_{zy} = 0, \quad \sigma_{zz} = r^\lambda$$

In order to obtain the order of singularity, he had to assume some loading distribution on the surface. Here this assumption shows that his results do not exactly satisfy free surface boundary conditions. Even though assuming this imaginary load, he could not satisfy the free surface boundary condition. Thus, finally he created additional solution for getting more degree of freedom. To achieve the additional solution, he introduced another coordinate, which is skew-symmetrical (spherical coordinate\*) to the plane  $z=0$  since he intended to remove the unwanted stress.

$$\text{Sol. D}^* = \text{sol. 7} \left\{ \psi_7 = r^{\lambda+1} \cos(\mu\varphi) P_{\lambda+1}^\mu(\cos\theta)/G \right\}$$

$$+ (\lambda + \mu + 1)(\lambda - \mu + 2) r^{\lambda+1} \cos(\mu - 2)\varphi P_{\lambda+1}^{\mu-2}(\cos\theta)/G \quad (\mu = 0, -1)$$

$$\text{Sol. E}^* = \text{sol. 7} \left\{ \psi_7 = r^{\lambda+1} \sin(\mu\varphi) P_{\lambda+1}^\mu(\cos\theta)/G \right\}$$

$$+ \frac{\mu(\lambda + \mu + 1)(\lambda - \mu + 2)}{\mu - 2} r^{\lambda+1} \sin(\mu - 2)\varphi P_{\lambda+1}^{\mu-2}(\cos\theta)/G \quad (\mu = -\frac{3}{2}, -\frac{5}{2})$$

## Stress intensity factor

Finally, he got five solution types(A,B,C,D\*,E\*) which is expressed in terms of eigenvalues. Through trial and error way in considering boundary condition, he can obtain eigenfunction for stresses and displacement corresponding to each eigenvalue. Here are some computed eigenvalues for the solution.

Poisson's ratio $\nu$	$\lambda$
0.0	-0.5
0.15	-0.4836
0.3	-0.4523
0.4	-0.4132
0.5	-0.3318
0.5	0.0
0.4	0.135
0.3	0.218
0.15	0.309
0.075	0.355
0.0	0.410
0.0	0.5
0.075	0.553
0.15	0.594
0.3	0.681
0.4	0.765
0.475	0.898
0.5	1.0

Fig 6 shows the non-zero stresses at the half-space surface( $z=0$ ) for poisson's ratio 0.5/0.3. It is remarkable that poisson's ratio is also significant factor for the stresses. The stresses are normalized such that at the crackfront  $z=1$ , the stress intensity factor factor  $k=\sqrt{2}$ .

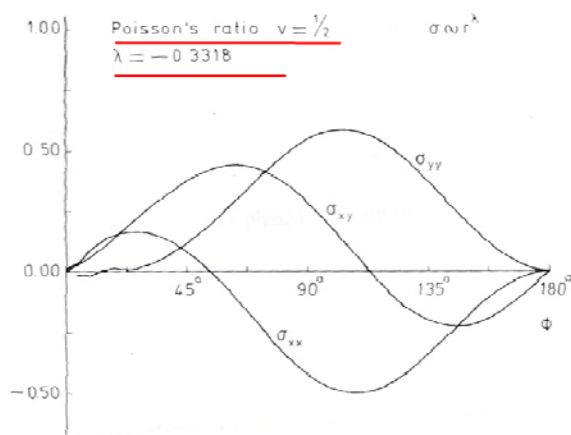


Fig 6. (a) Stress at  $z=0$ ,  $r=1$ . Stress Intensity Factor at the crack front at  $z=1$  is  $\sqrt{2}$ .  
Poisson's ratio=0.5

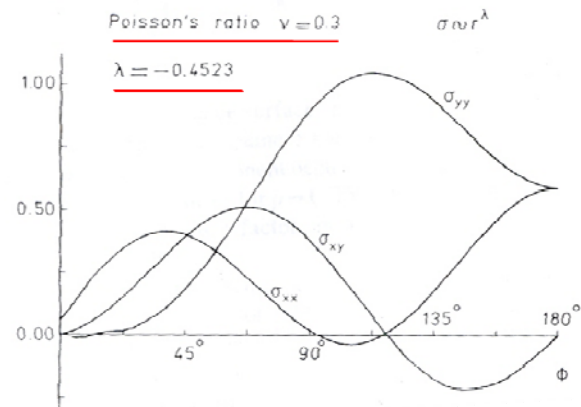


Fig 6. (b) Stress at  $z=0$ ,  $r=1$ . Stress Intensity Factor at the crack front at  $z=1$  is  $\sqrt{2}$ .  
Poisson's ratio=0.3

This indicates that stress  $\sigma_{yy}$  in the plane  $z=1$  behaves along the line  $\varphi = \pi$  is

$$\sigma_{yy} = \frac{k}{\sqrt{2\rho}} = \frac{1}{\sqrt{\rho}} \quad \rho \rightarrow 0$$

Here  $\rho$  is a horizontal distance from z-axis. Then express it in terms of  $\theta$

$$\sigma_{yy} = z^\lambda \frac{1}{\sqrt{\theta}} \quad \theta \rightarrow 0$$

Then from the relationship,

$$\sigma_{xx} = r^\lambda f_{xx}(\lambda, \theta, \varphi), \quad \sigma_{xy} = r^\lambda f_{xy}(\lambda, \theta, \varphi), \quad \dots$$

The above formula for other plane  $z=\text{const}$  becomes

$$\sigma_{yy} = z^{\lambda+1/2} \frac{1}{\sqrt{\rho}}$$

Then finally, we can get

$$\sigma_{yy} = \frac{k}{\sqrt{2\rho}} = z^{\lambda+1/2} \frac{1}{\sqrt{\rho}}$$

Therefore, stress intensity factor at the vertex is

$$k = \sqrt{2} z^{\lambda+1/2}$$

Hence at the half-space surface ( $z=0$ ) the stress-intensity factor is zero. This means that in the plane  $z=0$ , there are no stresses which vary according to  $\rho^{-1/2}$ . In other words, the result shows clearly the stress intensity factor for two-dimensional concept loses its meaning in the vertex. At this region, stress intensity factor essentially requires a three-dimensional one.

## Conclusion

First, ERRs, showing generally locally highest value in the center of the specimen varies along the crack line in case of a 3D model. This result is able to explain why a curved crack front occurs briefly, and moreover is observed that the averaged ERRs lie near the theoretical solution, showing a good agreement with analytic solution.

Then, through the observation of ERRs correspond to varying delamination lengths for a fixed width, we can see a relationship between width and delamination length. Relatively larger width than delamination length brings about the plane strain constraint. On the other hand, the constraint effect can be considered as a plane stress under the condition smaller or similar width when compared with crack length.

Finally, Benthem semi-analytic solution showed that stress intensity factor at the vertex does not follow the square-singular root any more. In the free surface plane( $z=0$ ), there are no stresses that vary according to  $\rho^{-1/2}$ . In other words, 2D stress-intensity factor loses its meaning in the vertex region. Additionally, we can see the poisson's ratio plays also a significant role in deciding stresses.

## Reference

- [1] Z. Suo, J. W. Hutchinson, 1989. Sandwich specimens for measuring interface crack toughness. *Mater. Sci. Eng.*, A107, 135–143.
- [2] I.S. Raju and K. N. Shivakumar , “Three Dimensional Elastic Analysis of a Composite double cantilever Beam Specimen”, *J. AIAA*, Vol26, 1988
- [3] J.P. Benthem, “State of Stress at the vertex of Quarter-Infinite Crack in a Half-Space”, *Int J. Solids Structure*, Vol.13, pp479-492,1977
- [4] J.P. Benthem, *J. of Elasticity* “ Note on the Boussinesq-Papkovich Stress Functions”, Vol. 9, 1978
- [5] Byerly, W. E. *An Elementary Treatise on Fourier's Series, and Spherical, Cylindrical, and Ellipsoidal Harmonics, with Applications to Problems in Mathematical Physics*. New York: Dover, p. 244, 1959.
- [6] Piero Villaggio, “ A Signorini Problem in Elasticity with Prescribed Contact Set”, *App. Math*, 1985